**Earthline Journal of Chemical Sciences**
ISSN (Online): 2581-9003
Volume 4, Number 1, 2020, Pages 35-51
https://doi.org/10.34198/ejcs.4120.3551

# 3(4)-Amino-4(3)-nitro-1,2,5-oxadiazole-2-oxides and their Ring-opened Isomers-A DFT Treatment

**Lemi Türker**

Department of Chemistry, Middle East Technical University, Üniversiteler, Eskişehir Yolu No: 1, 06800 Çankaya/Ankara, Turkey; e-mail: lturker@gmail.com; lturker@metu.edu.tr

## Abstract

Amino and nitro substituted 1,2,5-oxadiazole-2-oxide isomers and their ring-opened nitroso forms have been subjected to density functional treatment at the level of B3LYP/6-311++G(d,p). The transition states for the ring opening processes are obtained and the corresponding activation energies have been calculated. Also, 1,3- and 1,5-proton tautomerism yielding imine, oxime and *aci* forms are investigated. For all the structures, the stabilities, the HOMO, LUMO energies and the interfrontier molecular orbital energy gaps are obtained and the effects of substituents ($NH_2$ and $NO_2$) are discussed.

## Introduction

The furoxan (furazan oxide, 1,2,5-oxadiazole-2-oxide) ring system has been the subject of much debate and controversy since the first (unrecognized) preparation of a compound of this type in 1850's until almost the last decade of 19th century [1].

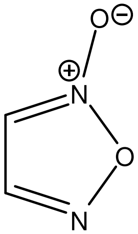

Received: February 29, 2020; Accepted: April 10, 2020

Keywords and phrases: furoxan, furazan oxide, 1,2,5-oxadiazole-2-oxide, pull-push, density functional, explosive.

Makhova and Fershtat, outlined recent advances in the synthesis and functionalization of 1,2,5-oxadiazole-2-oxides [2]. Some computational studies on structures having furoxan systems have been reported recently [3-6]. Some energetic compounds possessing 1,2,5-oxadiazole 2-oxide system have been reported [7]. 4,6-dinitrobenzofuroxan (DNBF) is one of those energetic compounds.

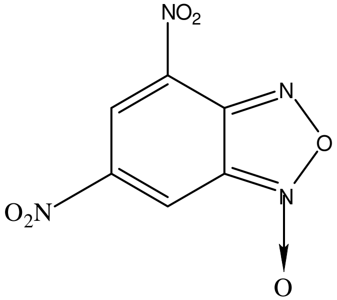

DNBF

Benzofuroxan and its derivatives exhibit interesting and challenging chemistry [8]. One of the striking behavior of BFO is its molecular rearrangement which involves 1,2-dinitroso benzene intermediate to yield the starting structure eventually.

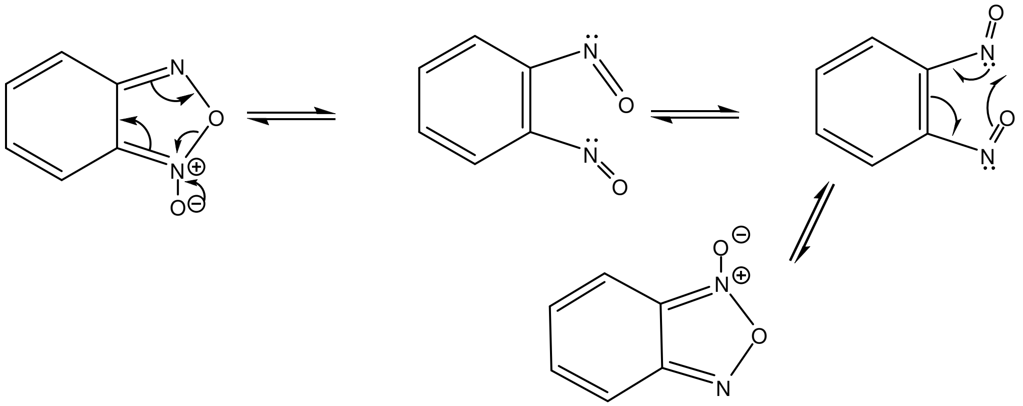

Pull-push type systems have interesting aspects. They have been investigated in various structures [9-15] and have some applications [16-17]. In DNBF structure shown above, the nitro groups are crossly conjugated whereas in the present 3(4)-amino-4(3)-nitro-1,2,5-oxadiazole-2-oxides (A and B), the amino and nitro groups are not directly conjugated with each other. However, they donate/accept electrons from the adjacent C=N bonds, causing some instability. To investigate those effects at the molecular level, presently some density functional (DFT) calculations have been performed.

A

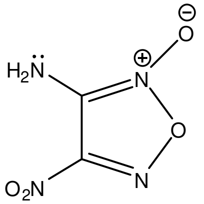

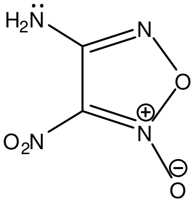

B

## Method of Calculation

The geometry optimizations of all the structures presently considered, leading to energy minima were achieved first by using MM2 method [18, 19] for the equilibrium conformer. Then, the subsequent optimizations were achieved at Hartree-Fock level using various basis sets hierarchically. Finally, the geometry optimizations were managed within the framework of density functional theory [20, 21] at the levels of RB3LYP/6-311++G(d,p). Note that the exchange term of B3LYP consists of hybrid Hartree-Fock and local spin density (LSD) exchange functions with Becke's gradient correlation to LSD exchange [21, 22]. Note that the correlation term of B3LYP consists of the Vosko, Wilk, Nusair (VWN3) local correlation functional [23] and Lee, Yang, Parr (LYP) correlation correction functional [24]. The vibrational analyses have also been done. The total electronic energies are corrected for the zero point vibrational energy (ZPE). The stationary points to energy minima were proved in all the cases by calculation of the second derivatives of energy with respect to the atom coordinates. The normal mode analysis for each structure yielded no imaginary frequencies for the $3N-6$ vibrational degrees of freedom, where $N$ is the number of atoms in the system. This indicates that the structure of each system corresponds to at least a local minimum on the potential energy surface. The transition states have been obtained at the same level of calculations and checked for single imaginary vibrational mode. All these calculations were done by using the Spartan 06 package program [25].

## Results and Discussion

Figure 1 shows the optimized structures of isomeric 3(4)-amino-4(3)-nitro-1,2,5-oxadiazole-2-oxides. The structures possess a potent embedded pull-push system generated by a nitro and an amino group linked to the oxadiazole ring system. Note that $NH_2$ and $NO_2$ groups in either oxadiazole-2-oxides (isomers A and B) are not directly conjugated. However, the pull-push action becomes apparent in the ring-opened dinitroso structures which have some resemblance to 1,1-diamino-2,2-dinitro ethylene (DADNE) also known as FOX-7, a well known explosive material. Structures A and B differ from each other in terms of the position of N-oxide moiety. The figure also shows the direction of the dipole moment vectors. Structures A and B have dipole moments of 3.190181 and 3.925416 debye, respectively.

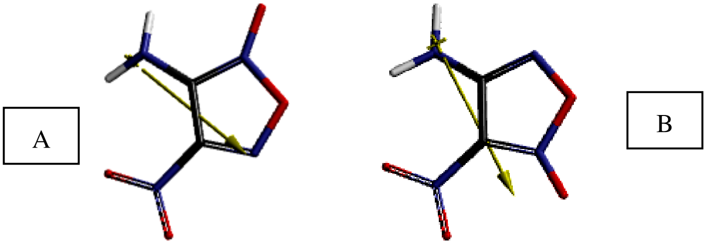

**Figure 1.** Optimized structure of the structures A and B.

Figure 2 shows the IR spectra of structures A and B. In the spectra the peaks above 3500 $cm^{-1}$ stand for symmetric and asymmetric N-H stretchings. The ring stretchings occur at 1729 $cm^{-1}$ and 1692 $cm^{-1}$ for A and B, respectively. The $NH_2$ scissoring of A is at 1629 $cm^{-1}$ coupled with asymmetric N-O stretching of the $NO_2$ group. In the case of B similar mode of vibrations occur at 1551 $cm^{-1}$. The huge peak at 1539 $cm^{-1}$ in the spectrum of A stands for various coupled vibrations. The peak at 1351 $cm^{-1}$ in the spectrum of B is the symmetrical $NO_2$ stretching and the ring vibrations overlapped with it.

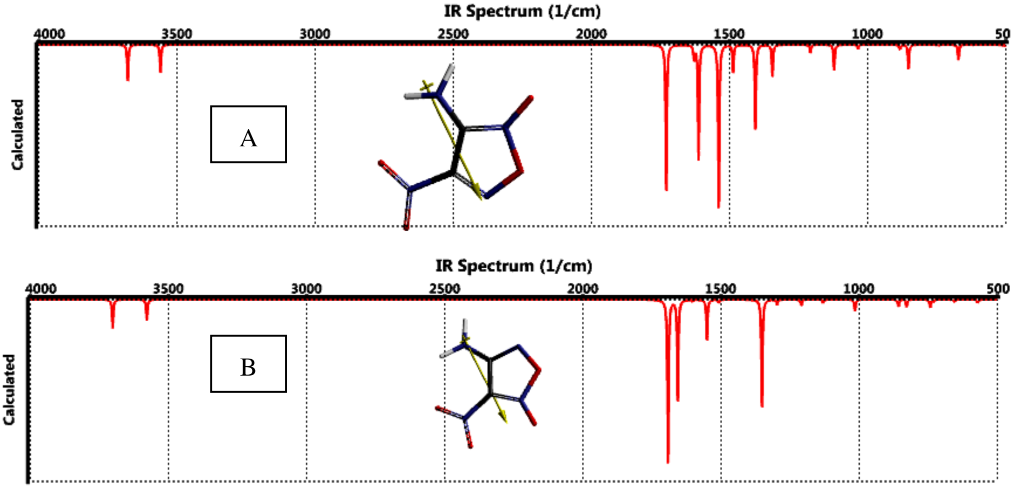

**Figure 2.** IR spectra of the cyclic structures considered.

Figure 3 displays the ESP charges on the atoms of isomers A and B. Note that ESP charges are obtained by the program based on a numerical method that generates charges that reproduce the electrostatic potential field from the entire wave function [25]. The charge distributions on A and B and the comparison reveal that the N-oxide moiety, nearby the amino group attracts some electron population from it. In another word, the amino group donates some electron population toward the C=N-O moiety. In structure B, the nitroso group attracts some electron population from C=N-O moiety.

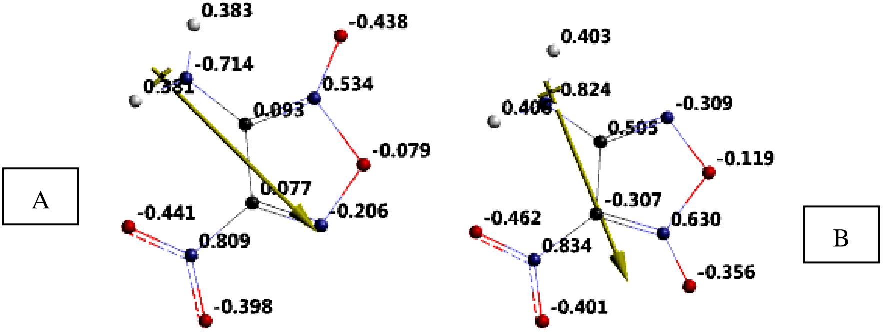

**Figure 3.** ESP charges on the atoms of structures A and B.

Figure 4 displays the electrostatic potential maps of structures A and B where red-reddish and blue-bluish regions stand for relatively electron rich and poor parts of the structures, respectively.

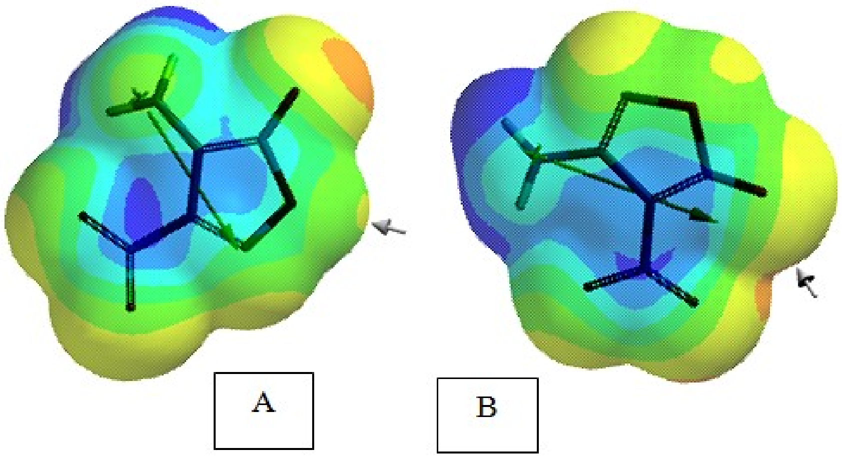

**Figure 4.** Electrostatic potential maps of structures A and B.

Table 1 presents the total electronic energy (E), zero point vibrational energy (ZPE) and the corrected total electronic energy ($E_c$) values of structures A and B. Namely, the nitro and N-oxide moieties on the same side of the structure yields a more stable molecule, relatively speaking A is less stable than B because of the following resonance structures.

**Table 1.** Some energies of the structures considered.

| Structure | E | ZPE | $E_c$ |
|---|---|---|---|
| A | -1568025.87 | 178.30 | -1567847.57 |
| B | -1568032.16 | 179.12 | -1567853.04 |

Energies in kJ/mol.

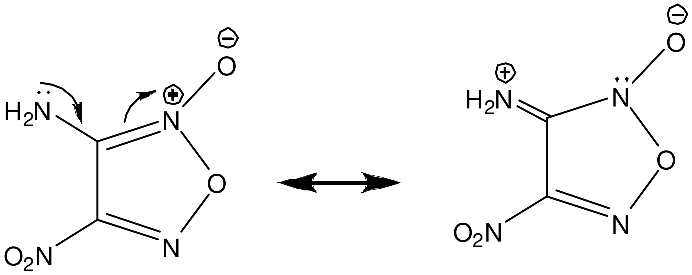

I

II

In structure II (related to structure A), firstly charge separation is further away from each other, hence raises up its energy. Secondly, it has lone-pair-negative charge assembly on 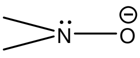 moiety which also raises up the energy due to repulsive interactions.

Figure 5 displays the time-dependent (TDDFT) UV-VIS spectra of A and B. Note that in A, chromophoric moieties ($NH_2$-C=N-O and $NO_2$-C=N) are not interacting with each other through resonance. So, in the spectrum of A, two well separated peaks appear. In structure B, $N^+$-$O^-$ moiety could be in conjugation with $NO_2$ group as well as with $NH_2$C=N group. Therefore, the peaks overlap in the spectrum of B. Apparently, compared to spectrum of A spectrum of B shows some hypsochromic effect.

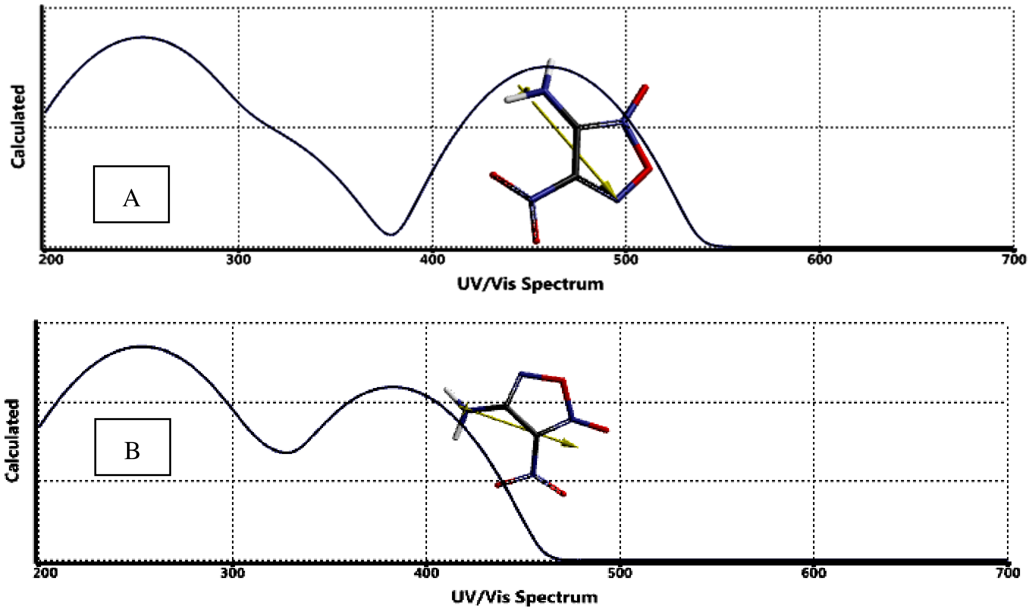

**Figure 5.** Time-dependent UV-VIS spectra of structures A and B.

## Ring-opened Structures

Figure 6 exhibits various conformers of the ring-opened structures originating from structures A and B. In C1 through C3, one or two of C-NO bonds had been locked prior to the optimization stage. As seen in the figure the directions of dipole moment vector is highly dependent on the conformation of NO groups. In structures C-C3, the amino and nitro groups are in conjugation with nitroso groups in various ways. The amino group donates electrons in to the conjugative system. That is why the positive end of dipole vector lies on the $NH_2$ group.

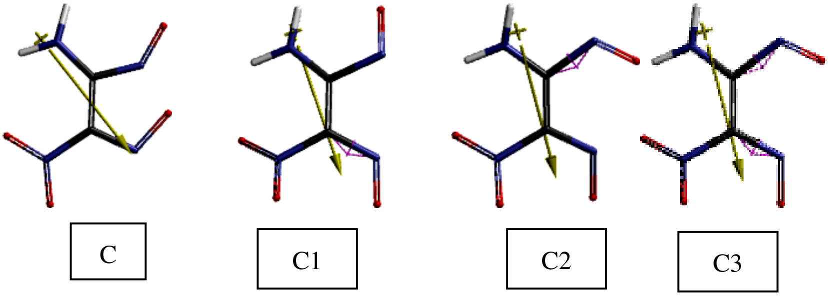

**Figure 6.** Optimized structures of various conformers of the ring-opened structures.

Figure 7 shows the IR spectra of the ring-opened structures. In the spectra the peaks at and above 3500 cm$^{-1}$ are symmetrical and asymmetrical N-H stretchings. In the spectrum of C, C-NH$_2$ and C-NO stretchings occur at 1730 cm$^{-1}$. In all the spectra various vibrations happen in between 1750 and 1500 cm$^{-1}$ having a quite similar pattern.

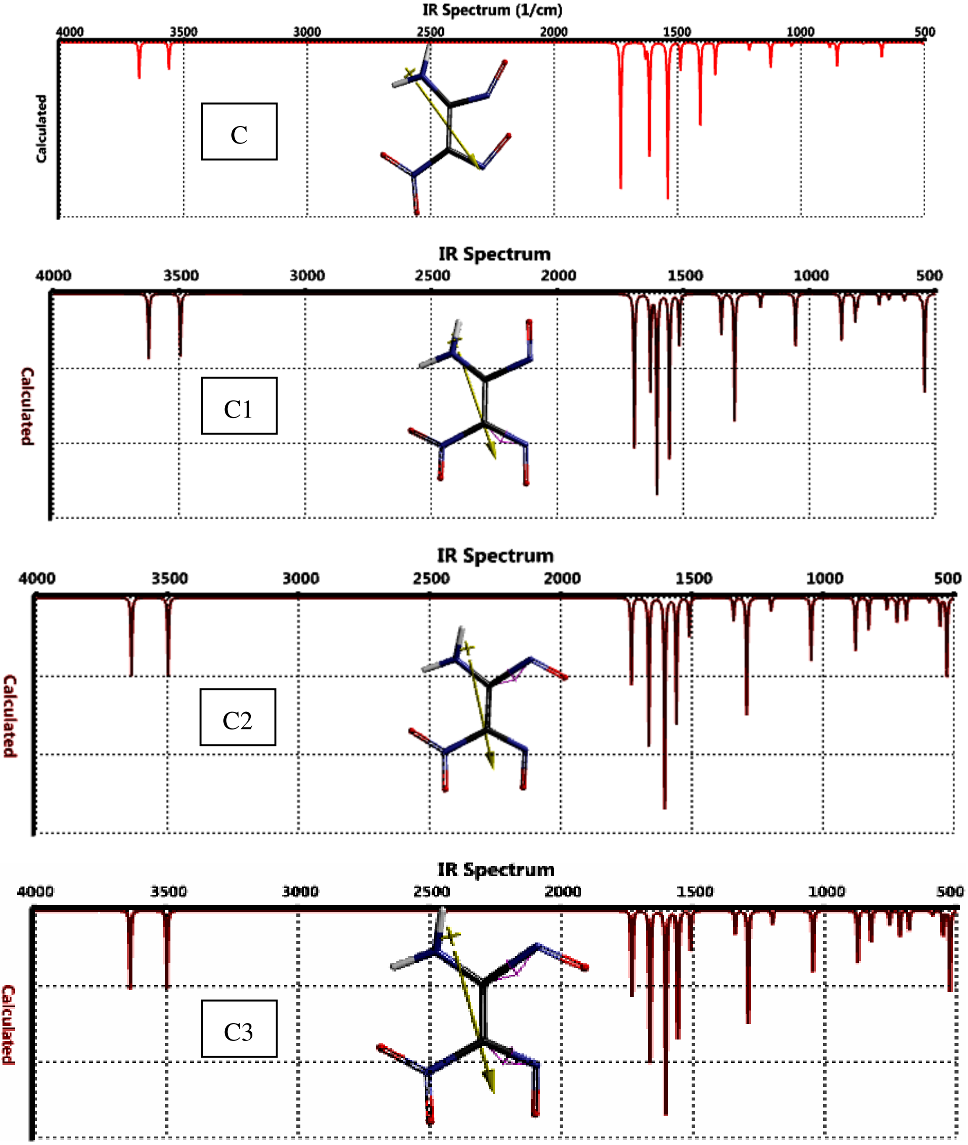

**Figure 7.** IR spectra of various conformers of the ring-opened structures considered.

Table 2 shows various energies of the ring-opened structures which are all enamine structures. Conformer C which possesses no constraint is the most stable of all. On the other hand, all the ring-opened structures are isoconjugate with an even alternant hydrocarbon [26, 27] dianion. Certain centric perturbations [26, 27] on it yield the ring-opened isomers of structures A and B presently considered. Note that the present alternant hydrocarbon dianion is a non-Kekule' structure having six starred and four unstarred positions [26-28]. Note also that an existence of a non-Kekule' molecular structure is necessary but not a sufficient condition for being an explosive molecule. The dinitroso structures considered partially resemble DEADNE (FOX-7). One of each $NH_2$ and $NO_2$ groups of FOX-7 has been replaced by the nitroso groups in the dinitroso structures considered. Fox-7 is also isoconjugate with a non-Kekule' even alternant hydrocarbon system having seven stared and three unstarred positions.

**Table 2.** Some energies of the conformers of ring-opened structures considered.

| Structure | E | ZPE | $E_c$ |
|---|---|---|---|
| C | -1568026.03 | 178.51 | -1567847.52 |
| C1 | -1567963.41 | 170.44 | -1567792.96 |
| C2 | -1567938.08 | 169.24 | -1567768.84 |
| C3 | -1567937.98 | 169.22 | -1567768.76 |

Energies in kJ/mol.

## Transitions

Figure 8 shows the transition state geometries of structures A and B during the ring opening process. Those structures are labeled as A-CA and B-CB. The leftmost letter in the labeling stands for the initial structure, letter C indicates relative conformation of the nitroso groups and the last letter specifies the transition state considered.

Figure 9 displays the IR spectra of the transition states considered. In the spectra rather weak N-H stretchings occur at and above 3500 $cm^{-1}$. In the spectrum of A-CA, the nitroso N=O stretching occurs at 1678 $cm^{-1}$ followed by asymmetrical $NO_2$ stretchings at 1630 $cm^{-1}$. In B-CB spectrum C-NO stretching appears at 1714 $cm^{-1}$ as a sharp strong peak followed by asymmetrical $NO_2$ stretchings at 1606 $cm^{-1}$. Whereas the symmetrical ones happen at 1365 $cm^{-1}$.

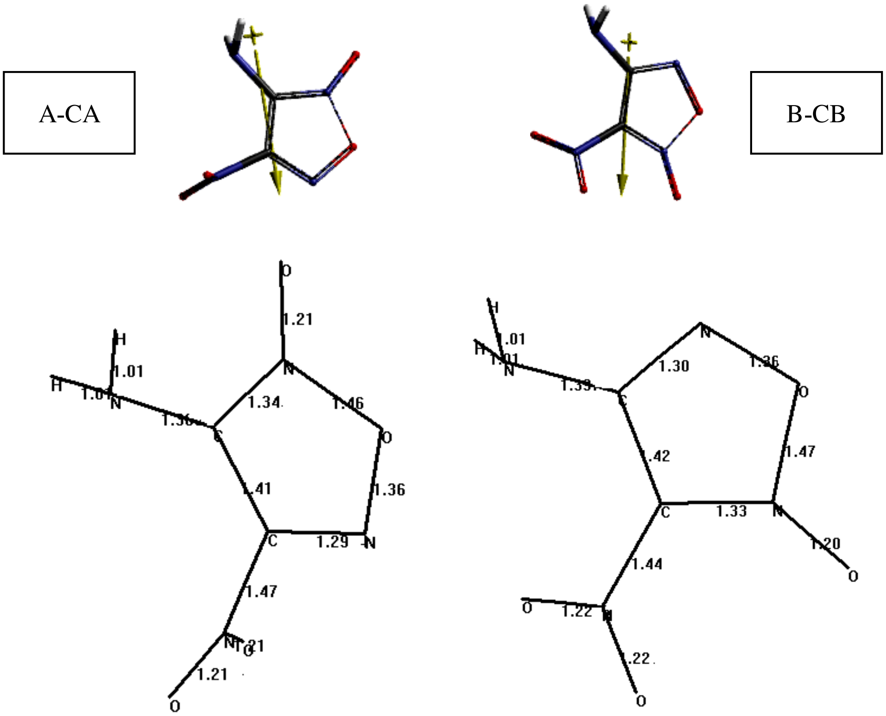

**Figure 8.** The transition state geometries of structures A and B (Bond lengths in Ǻ).

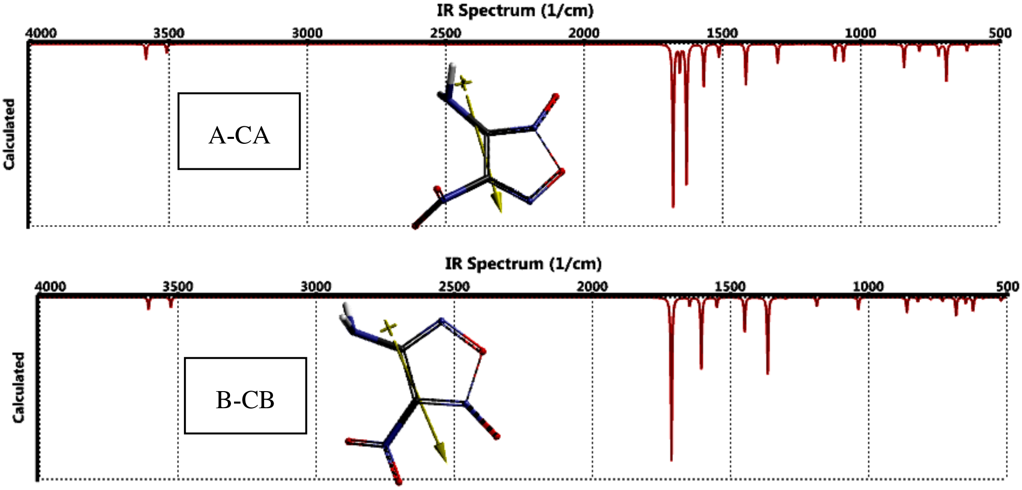

**Figure 9.** IR spectra of the transition states considered.

Table 3 includes some energies of the transition states. Transition state A-CA is more stable than B-CB. The corresponding activation energies for the ring opening reactions are 33.57 kJ/mol and 45.34 kJ/mol, respectively. Note that $E_c$ values of C2 and C3 are close to each other (see Table 2). In calculating the activation energies for B-CB transition, $E_c$ value of C2 is considered because it is more stable than C3 (C2 possesses less constraint!).

**Table 3.** Some energies of the transition states.

| Transition | E | ZPE | $E_c$ |
|---|---|---|---|
| A-CA | -1567990.74 | 176.735061 | -1567814.00 |
| B-CB | -1567984.61 | 176.910314 | -1567807.70 |

Energies in kJ/mol

### Tautomers

The ring-opened dinitroso structures considered are capable of undergoing 1,3- and 1,5-type proton tautomerism. The 1,3-type proton shift leads to an imine structure (imine-enamine tautomerism) whereas 1,5-type results in oxime (nitroso-oxime tautomerism) and *aci*-forms (nitro-*aci* tautomerism).

Figure 10 shows the optimized structures of the proton tautomers of ring-opened structure-C considered.

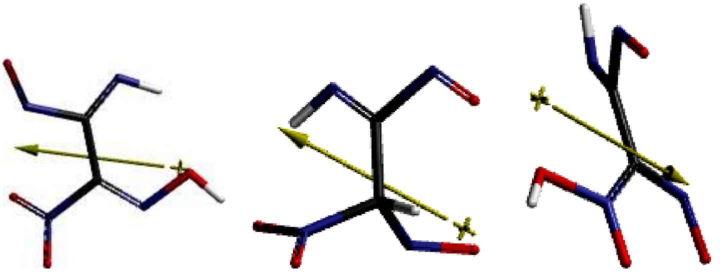

Oxime form

Imine form

*Aci* form

**Figure 10.** Optimized structures of some tautomeric forms of structure-C.

Figure 11 displays the IR spectra of the tautomers considered. The oxime form has N-H and O-H stretchings at 3493 $cm^{-1}$ and 3791 $cm^{-1}$, respectively. The sharp and strong peak at 1621 $cm^{-1}$ is for asymmetrical $NO_2$ stretchings.

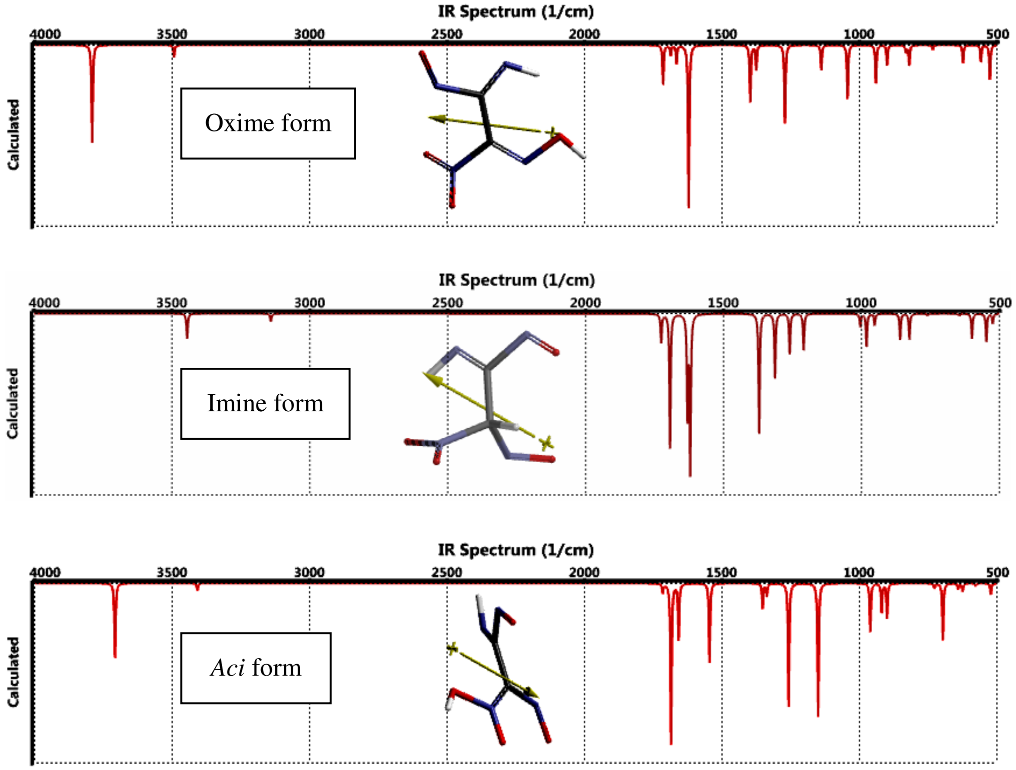

**Figure 11.** IR spectra of the tautomers considered.

The IR spectra of the imine form is characterized with a weak N-H stretching at 3445 $cm^{-1}$ which is followed by a very weak C-H stretching at 3141 $cm^{-1}$. The peaks grouped at 1500-1700 $cm^{-1}$ stand for various coupled vibrations.

The spectrum of *aci* form exhibits medium O-H stretching at 3708 $cm^{-1}$. The N-H stretching occurs at 3408 $cm^{-1}$ as a weak peak. At 1685 $cm^{-1}$ bending of O-H and C-N stretching of *aci* group coupled together. The N=O stretchings occur at 1657 $cm^{-1}$ and 1545 $cm^{-1}$.

The data in Table 4 indicates that the oxime form is more stable than the others. Note that both of the oxime and *aci* forms are 1,5-type tautomers. The greater stability of the oxime form can be attributed to transoid conformation of HN=C-C=NOH moiety as well as some hydrogen bond formation between the NH and OH groups present.

**Table 4.** Some energies of the tautomeric structures considered.

| Structure | E | ZPE | $E_c$ |
|---|---|---|---|
| Imine | -1567899.86 | 168.22 | -1567731.64 |
| Oxime | -1567955.43 | 173.03 | -1567782.40 |
| *Aci* | -1567879.28 | 166.88 | -1567712.40 |

Energies in kJ/mol.

All the structures presently considered are isomeric. The stability order of them is *aci*-form<imine form<C3<C2<oxime form<C1<C<A<B. Note that all the C-series of structures are in the enamine form.

## Frontier Molecular Orbital Energies

Table 5 shows the HOMO, LUMO energies and the interfrontier molecular orbital energy gaps (Δε) of the structures considered. Of the structurally related isomers A and B, the former one has higher HOMO but lower LUMO energies compared to respective energies of B, so that A possesses narrower interfrontier molecular orbital energy gap. It is known that impact sensitivity of an explosive material increases as Δε value gets smaller and smaller [29]. In that sense, structure A should be more sensitive than its isomer B. In the case of ring-opened structures, the order of HOMO and LUMO energies are C<C1<C2<C3 and C1<C2<C3<C, respectively. Their Δε values follow the order of C>C1>C3>C2. These orders mentioned above are dictated by conformation of the groups linked to the conjugative path, thus depends on the extent of conjugation. As for the tautomers, the imine form, which is a 1,3-type tautomer, has lower HOMO and LUMO energies compared to other tautomers of 1,5-type. Their Δε values follow the order of imine form>oxime form>*aci* form.

**Table 5.** The HOMO, LUMO energies and the interfrontier energy gaps of the structures considered.

| Structure | HOMO | LUMO | Δε |
|---|---|---|---|
| A | -685.86 | -378.40 | 307.46 |
| B | -735.56 | -368.69 | 366.87 |
| C | -685.56 | -378.30 | 307.26 |
| C1 | -657.42 | -471.16 | 186.26 |
| C2 | -633.32 | -462.80 | 170.52 |
| C3 | -633.01 | -462.32 | 170.69 |
| Imine form | -750.50 | -436.81 | 313.69 |
| Oxime form | -691.94 | -393.15 | 298.79 |
| *Aci* form | -673.69 | -411.23 | 262.46 |

Energies in kJ/mol.

## Conclusion

The presently performed DFT calculations at the level of B3LYP/6-311++G(d,p) reveal that the furoxan structures considered are stable such that $NO_2$ group nearby the N-oxide moiety (structure B) is more stable than the one having the amino group and the N-oxide moiety close to each other (structure A). These N-oxides considered are capable of undergoing ring-opening and forming dinitroso isomers. In those transformations, structure A requires less activation energy as compared to structure B. The ring opened structures may exhibit proton tautomerism. All the nitroso as well as the tautomeric forms are less stable than the furoxans (A and B) considered presently.

## References

[1] N. Wang, B. Chen and Y. Ou, Review on benzofuroxan system compounds, *Propellants, Explosives, Pyrotechnics* 19 (1994), 145-148. https://doi.org/10.1002/prep.19940190306 (A. Kekule, *Justus Liebigs Ann. Chem.* 101, 200 (1857); 105, 279 (1858)).

[2] N. N. Makhova and L. L. Fershtat, Recent advances in the synthesis and functionalization of 1,2,5-oxadiazole 2-oxides, *Tetrahedron Letters* 59(24) (2018), 2317-2326. https://doi.org/10.1016/j.tetlet.2018.04.070

[3] L. Türker, Furoxan derivatives of pyrene - a DFT study, *Polycyclic Aromatic Compounds* 38(3) (2018), 257-271. https://doi.org/10.1080/10406638.2016.1200637

[4] L. Türker, Isomerization of 4,6-dinitrobenzofuroxan - a DFT study, *Journal of Energetic Materials* 29(2) (2011), 127-149. https://doi.org/10.1080/07370652.2010.510496

[5] L. Türker, C. C. Bayar and A. T. Balaban, A DFT study on push-pull (amino-nitro) fulminenes and hexahelicenes, *Polycyclic Aromatic Compounds* 30(2) (2010), 91-111. https://doi.org/10.1080/10406631003756005

[6] L. Türker, A DFT study on benzotrifuroxan and its isomers, *Polycyclic Aromatic Compounds* 30(1) (2010), 44-60. https://doi.org/10.1080/10406631003608479

[7] Z. Xu, H. Yang and G. Cheng, Novel energetic compounds based on 3-methyl-1,2,5-oxadiazole 2-oxide, *Journal of Energetic Materials* 36(1) (2018), 29-37. https://doi.org/10.1080/07370652.2017.1302519

[8] A. R. Katritzky and M. F. Gordeev, Heterocyclic rearrangements of benzofuroxanes and related compounds. A review about the chemistry of benzofuroxans, *Heterocycles* 35 (1993), 483-518. https://doi.org/10.3987/REV-92-SR2

[9] M. S. Morales-Ríos, M. García-Velgara, H. Cervantes-Cuevas, C. Alvarez-Cisneros and P. Joseph-Nathan, Push-pull and pull-push effects in isatylidenes, *Magnetic Resonance in Chemistry* 38(3) (2000), 172-176. https://doi.org/10.1002/(SICI)1097-458X(200003)38:3%3C172::AID-MRC618%3E3.0.CO;2-D

[10] A. Sutter, P. Retailleau, W. C. Huang, H. W. Lin and R. Ziessel, Photovoltaic performance of novel push-pull-push thienyl-Bodipy dyes in solution-processed BHJ-solar cells, *New Journal of Chemistry* 38(4) (2014), 1701-1710. https://doi.org/10.1039/C3NJ01436C

[11] L. Türker, Interaction of TATB with Cu and $Cu^{+1}$. A DFT study, *Defence Technology* 15(1) (2019), 27-37. https://doi.org/10.1016/j.dt.2018.05.001

[12] R. Kundu and C. Kulshreshtha, Design, synthesis and electronic properties of push-pull type dye, *RSC Advances* 5(94) (2015), 77460-77468. https://doi.org/10.1039/C5RA13416A

[13] B. Sekaran, Y. Jang, R. Misra and F. D’Souza, Push-pull porphyrins via β-pyrrole functionalization: evidence of excited state events leading to high-potential charge-

separated states, *Chemistry - A European Journal* 25(56) (2019), 12991-13001. https://doi.org/10.1002/chem.201902286

[14] J. T. Ye, H. Q. Wang, Y. Zhang and Y. Q. Qiu, Regulation of the molecular architectures on second-order nonlinear optical response and thermally activated delayed fluorescence property: homoconjugation and twisted donor-acceptor, *Journal of Physical Chemistry C* (2020), to appear.

[15] T. Duan, R. Z. Liang, Y. F. Pai, K. Wang, C. Zhong, S. Lu and D. Yu, Facile synthesis of bis-dicyanovinylidene-end-capped push-pull molecules as panchromatic absorbers, *Dyes and Pigments* 161 (2019), 227-232. https://doi.org/10.1016/j.dyepig.2018.09.060

[16] C. Kumar, A. A. Raheem, K. Pandian, R. Shanmugam and C. Praveen, Fine-tuning the optoelectronic chattels of fluoreno-thiophene centred molecular semiconductors through symmetric and asymmetric push-pull switch, *New Journal of Chemistry* 43(18) (2019), 7015-7027. https://doi.org/10.1039/C9NJ00775J

[17] E. V. Verbitskiy, A. A. Baranova, K. I. Lugovik, K. O. Khokhlov, E. M. Cheprakova, G. L. Rusinov, O. N. Chupakhin and V. N. Charushin, New V-shaped push-pull systems based on 4,5-di(hetero)aryl substituted pyrimidines: their synthesis and application to the detection of nitroaromatic explosives, *Arkivoc* 3 (2016), 360-373.| https://doi.org/10.3998/ark.5550190.p009.470

[18] A. R. Leach, *Molecular Modeling*, Essex: Longman, 1997.

[19] P. Fletcher, *Practical Methods of Optimization*, New York: Wiley, 1990.

[20] W. Kohn and L. J. Sham, Self-consistent equations including exchange and correlation Effects, *J. Phys. Rev.* 140 (1965), 1133-1138. https://doi.org/10.1103/PhysRev.140.A1133

[21] R. G. Parr and W. Yang, *Density Functional Theory of Atoms and Molecules*, London: Oxford University Press, 1989.

[22] A. D. Becke, Density-functional exchange-energy approximation with correct asymptotic behavior, *Phys. Rev. A* 38 (1988), 3098-3100. https://doi.org/10.1103/PhysRevA.38.3098

[23] S. H. Vosko, L. Wilk and M. Nusair, Accurate spin-dependent electron liquid correlation energies for local spin density calculations: a critical analysis, *Can. J. Phys.* 58 (1980), 1200-1211. https://doi.org/10.1139/p80-159

[24] C. Lee, W. Yang and R. G. Parr, Development of the Colle-Salvetti correlation-energy formula into a functional of the electron density, *Phys. Rev. B* 37 (1988), 785-789. https://doi.org/10.1103/PhysRevB.37.785

[25] SPARTAN 06, Wavefunction Inc., Irvine CA, USA, 2006.

[26] M. J. S. Dewar, *The Molecular Orbital Theory of Organic Chemistry*, New York: McGraw-Hill, 1969.

[27] M. J. S. Dewar and R. C. Dougherty, *The PMO Theory of Organic Chemistry*, NY: Plenum-Rosetta, 1975. https://doi.org/10.1007/978-1-4613-4404-9

[28] L. Türker, Recent developments in the theory of explosive materials, in: *Explosive Materials*, J.T. Jansen, ed., New York: NOVA, 2011.

[29] N. R. Badders, C. Wei, A. A. Aldeeb, W. J. Rogers and M. S. Mannan, Predicting the impact sensitivity of polynitro compounds using quantum chemical descriptors, *J. Energetic Materials* 24 (2006), 17-33. https://doi.org/10.1080/07370650500374326.